

Projection-free Graph-based Classifier Learning using Gershgorin Disc Perfect Alignment

Cheng Yang,¹ Gene Cheung,² Guangtao Zhai³

¹ Shanghai University of Electric Power, Shanghai, China

² York University, Toronto, Canada

³ Shanghai Jiao Tong University, Shanghai, China

cheng.yang@shiep.edu.cn, genec@yorku.ca, zhaiguangtao@sjtu.edu.cn

Abstract

In semi-supervised graph-based binary classifier learning, a subset of known labels \hat{x}_i are used to infer unknown labels, assuming that the label signal \mathbf{x} is smooth with respect to a similarity graph specified by a Laplacian matrix. When restricting labels x_i to binary values, the problem is NP-hard. While a conventional semi-definite programming relaxation (SDR) can be solved in polynomial time using, for example, the alternating direction method of multipliers (ADMM), the complexity of projecting a candidate matrix \mathbf{M} onto the positive semi-definite (PSD) cone ($\mathbf{M} \succeq 0$) per iteration remains high. In this paper, leveraging a recent linear algebraic theory called Gershgorin disc perfect alignment (GDPA), we propose a fast projection-free method by solving a sequence of linear programs (LP) instead. Specifically, we first recast the SDR to its dual, where a feasible solution $\mathbf{H} \succeq 0$ is interpreted as a Laplacian matrix corresponding to a balanced signed graph minus the last node. To achieve graph balance, we split the last node into two, each retains the original positive / negative edges, resulting in a new Laplacian $\tilde{\mathbf{H}}$. We repose the SDR dual for solution $\tilde{\mathbf{H}}$, then replace the PSD cone constraint $\tilde{\mathbf{H}} \succeq 0$ with linear constraints derived from GDPA—sufficient conditions to ensure $\tilde{\mathbf{H}}$ is PSD—so that the optimization becomes an LP per iteration. Finally, we extract predicted labels from converged solution $\tilde{\mathbf{H}}$. Experiments show that our algorithm enjoyed a $28 \times$ speedup over the next fastest scheme while achieving comparable label prediction performance.

Introduction

Binary classification—assignment of labels $\mathbf{x} \in \{-1, 1\}^N$ to an N -sample set to separate two distinct classes—is a basic machine learning problem (Bishop 2006). One common setting is semi-supervised graph classifier learning: use M known labels, $\hat{x}_i, 1 \leq i \leq M$, to infer $N - M$ unknown labels $x_i, M + 1 \leq i \leq N$, assuming that \mathbf{x} is smooth with respect to (w.r.t.) a similarity graph \mathcal{G} specified by a graph Laplacian matrix \mathbf{L} (Zhou et al. 2003; Belkin, Matveeva, and Niyogi 2004; Guillory and Bilmes 2009). This binary graph classifier problem is NP-hard (Luo et al. 2010).

Semi-definite programming (SDP) relaxation (SDR) (Li, Liu, and Tang 2008) is known to provide good error-bounded approximations to *quadratically constrained quadratic programs* (QCQP), of which binary graph classification is a

Preprint. Under review.

special case (See Table I and II in (Luo et al. 2010)). In a nutshell, SDR replaces the binary label constraint with a more relaxed *positive semi-definite* (PSD) cone constraint (*i.e.*, matrix variable \mathbf{M} related to $\mathbf{x}\mathbf{x}^\top$ satisfying $\mathbf{M} \succeq 0$). The relaxed problem can be solved in polynomial time using, for example, the *alternating direction method of multipliers* (ADMM) (O’Donoghue et al. 2016). However, ADMM still requires projection to the PSD cone $\mathcal{S} = \{\mathbf{M} \mid \mathbf{M} \succeq 0\}$ per iteration, which is expensive ($\mathcal{O}(N^3)$) due to full-matrix eigen-decomposition. An alternative approach removes the binary constraint and minimizes directly a quadratic graph smoothness term called *graph Laplacian regularization* (GLR) $\mathbf{x}^\top \mathbf{L} \mathbf{x}$ (Pang and Cheung 2017) for $\mathbf{x} \in \mathbb{R}^N$, then rounds x_i ’s to nearest binary values $\{-1, 1\}$. However, spectral methods such as GLR do not have tight performance bounds common in SDR (Goemans and Williamson 1995).

To ensure matrix variable \mathbf{M} is PSD without eigen-decomposition, one naïve approach is to enforce linear constraints derived directly from the *Gershgorin circle theorem* (GCT) (Varga 2004). By GCT, every real eigenvalue λ of a real symmetric matrix \mathbf{M} resides inside at least one *Gershgorin disc* Ψ_i —corresponding to row i of \mathbf{M} —with center $c_i(\mathbf{M}) \triangleq M_{i,i}$ and radius $r_i(\mathbf{M}) \triangleq \sum_{j \neq i} |M_{i,j}|$, *i.e.*,

$$c_i(\mathbf{M}) - r_i(\mathbf{M}) \leq \lambda \leq c_i(\mathbf{M}) + r_i(\mathbf{M}), \quad \exists i. \quad (1)$$

The corollary is that the smallest eigenvalue, $\lambda_{\min}(\mathbf{M})$, of \mathbf{M} is lower-bounded by the smallest Gershgorin disc left-end, denoted by $\lambda_{\min}^-(\mathbf{M})$, *i.e.*,

$$\lambda_{\min}^-(\mathbf{M}) \triangleq \min_i c_i(\mathbf{M}) - r_i(\mathbf{M}) \leq \lambda_{\min}(\mathbf{M}). \quad (2)$$

Thus, to ensure $\mathbf{M} \succeq 0$, one can impose the sufficient condition $\lambda_{\min}^-(\mathbf{M}) \geq 0$. While replacing the PSD cone constraint with a set of N linear constraints, $c_i(\mathbf{M}) - r_i(\mathbf{M}) \geq 0, \forall i$, is attractive computationally, GCT lower bound $\lambda_{\min}^-(\mathbf{M})$ tends to be loose. As an example, consider the *positive definite* (PD) matrix \mathbf{M} in Fig. 1(a) with $\lambda_{\min}(\mathbf{M}) = 0.1078$. The first Gershgorin disc left-end is $c_1(\mathbf{M}) - r_1(\mathbf{M}) = 2 - 3 = -1$, and $\lambda_{\min}^-(\mathbf{M}) < 0$. Thus, imposing $\lambda_{\min}^-(\mathbf{M}) \geq 0$ directly would aggressively restrict the search space, resulting in a sub-optimal solution to the posed problem.

A recent linear algebraic theory called *Gershgorin disc perfect alignment* (GDPA) (Yang, Cheung, and Hu 2021) provides a theoretical foundation to tighten the GCT lower

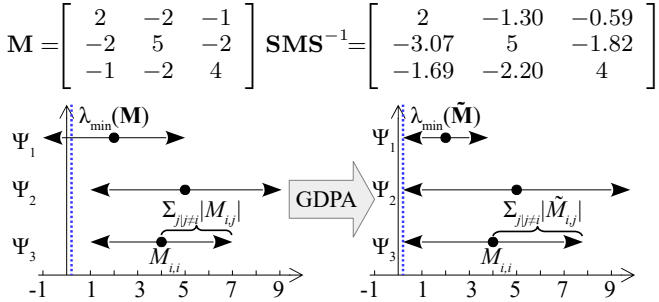


Figure 1: Example of a PD matrix \mathbf{M} and its similarity transform $\tilde{\mathbf{M}} = \mathbf{SMS}^{-1}$, and their respective Gershgorin discs Ψ_i . Note that Gershgorin disc left-ends of $\tilde{\mathbf{M}}$ are aligned at $\lambda_{\min}(\mathbf{M}) = 0.1078$.

bound. Specifically, GDPA states that given a graph Laplacian matrix \mathbf{L} corresponding to a *balanced* signed graph \mathcal{G} (Cartwright and Harary 1956), one can perform a *similarity transform*¹, $\tilde{\mathbf{L}} = \mathbf{SLS}^{-1}$, where $\mathbf{S} = \text{diag}(v_1^{-1}, \dots, v_N^{-1})$ and \mathbf{v} is the first eigenvector of \mathbf{L} , such that all Gershgorin disc left-ends of $\tilde{\mathbf{L}}$ are *exactly* aligned at $\lambda_{\min}(\mathbf{L}) = \lambda_{\min}(\tilde{\mathbf{L}})$. Thus, transformed $\tilde{\mathbf{L}}$ satisfies $\lambda_{\min}^-(\tilde{\mathbf{L}}) = \lambda_{\min}^+(\tilde{\mathbf{L}})$; *i.e.*, the *GCT lower bound is the tightest possible after an appropriate similarity transform*. Continuing our example, similarity transform $\tilde{\mathbf{M}} = \mathbf{SMS}^{-1}$ has all its disc left-ends exactly aligned at $\lambda_{\min}(\mathbf{M}) = \lambda_{\min}(\tilde{\mathbf{M}}) = 0.1078$.

Leveraging GDPA, we develop a fast projection-free algorithm for semi-supervised graph classifier learning. We first derive an SDR formulation for matrix solution \mathbf{M} from the original graph classifier problem. However, solution \mathbf{M} is not a Laplacian to a balanced graph, as required by GDPA. Thus, we convert the problem to its SDR dual (Gartner and Matousek 2012) and interpret the dual variable \mathbf{H} as a Laplacian to a balanced graph *minus* the last graph node. To achieve graph balance, we split the last node into two and divide the original positive and negative edges between them, resulting in a revised Laplacian $\tilde{\mathbf{H}}$. We repose the SDR dual problem for solution $\tilde{\mathbf{H}}$, then replace the PSD cone constraint $\tilde{\mathbf{H}} \succeq 0$ with linear constraints derived from GDPA. This changes the optimization to a *linear program* (LP) per iteration, which is solved efficiently using a fast LP solver (Vanderbei 2021). Finally, we extract prediction labels from converged solution $\tilde{\mathbf{H}}$. Experiments show that our algorithm enjoyed 28× speedup on average over the next fastest scheme, while retaining comparable label prediction performance.

Related Work

Graph-based classification was first studied two decades ago (Zhou et al. 2003; Belkin, Matveeva, and Niyogi 2004; Gulyáry and Bilmes 2009). With the advent of *graph signal processing* (GSP) (Ortega et al. 2018; Cheung et al. 2018a)—analysis of discrete signals residing on finite graphs—interest in the problem was revived (Gavish, Nadler, and Coifman 2010; Shuman, Faraji, and Vandergheynst 2011; Cheung et al.

¹A similarity transform $\mathbf{B} = \mathbf{SAS}^{-1}$ and the original matrix \mathbf{A} share the same set of eigenvalues (Varga 2004).

2018b). The problem of learning a similarity graph from data has been extensively studied (Dong et al. 2019). We focus on the orthogonal problem of predicting binary labels given a graph and a subset of M labels.

SDR—useful in approximating NP-hard problems (Gartner and Matousek 2012) such as QCQP—provides an effective relaxation to the binary graph classifier problem (Li, Liu, and Tang 2008). An interior point method tailored for the slightly more general *binary quadratic problem*² (BQP) has complexity $\mathcal{O}(N^{3.5} \log(1/\epsilon))$, where ϵ is the tolerable error (Helmburg et al. 1996). The complexity was improved to $\mathcal{O}(N^3)$ by SDCut (Wang, Shen, and van den Hengel 2013; Wang et al. 2017) via spectrahedron-based relaxation. Replacing the PSD cone constraint $\mathbf{M} \succeq 0$ with a factorization $\mathbf{M} = \mathbf{XX}^\top$ was proposed in (Shah et al. 2016), but resulted in a non-convex optimization for \mathbf{X} that was minimized locally, where in each iteration a matrix inverse of worst-case complexity $\mathcal{O}(N^3)$ was required. More recent first-order methods for SDP such as (O’Donoghue et al. 2016) used ADMM (Boyd et al. 2011; Zheng, Fantuzzi, and Papachristodoulou 2019; Zheng et al. 2020), but the iterative projection onto PSD cone requires full-matrix eigen-decomposition and thus expensive. In contrast, leveraging GDPA theory (Yang, Cheung, and Hu 2021), our algorithm is entirely projection-free.

It is known in graph spectral theory (Chung 1996) that balanced signed graphs have unique spectral properties (Dittrich and Matz 2020); for example, the *signed graph Laplacian matrix* (Kunegis et al. 2010) has eigenvalue 0 iff the underlying graph is balanced. In contrast, GDPA (Yang, Cheung, and Hu 2021) states that all Gershgorin disc left-ends of a similarity transform \mathbf{SMS}^{-1} of graph Laplacian \mathbf{M} to a balanced graph can be perfectly aligned at $\lambda_{\min}(\mathbf{M})$. GDPA theory was developed for fast *metric learning* (Moutafis, Leng, and Kakadiaris 2017) to optimize a PD matrix \mathbf{M} given a convex and differentiable objective $Q(\mathbf{M})$.

While also leveraging GDPA, this work addresses the binary graph classification problem in a different and non-trivial manner. Specifically, observing that solution \mathbf{H} to the SDR dual is a Laplacian to a balanced graph \mathcal{G} minus the last node, we augment the last node to obtain an overall balanced graph $\tilde{\mathcal{G}}$ via new Lemma 1, and solve a modified SDR dual for Laplacian $\tilde{\mathbf{H}}$ to $\tilde{\mathcal{G}}$ via GDPA linearization.

Preliminaries

Graph Definitions

A graph $\mathcal{G}(\mathcal{V}, \mathcal{E}, \mathbf{W})$ has node set $\mathcal{V} = \{1, \dots, N\}$ and edge set $\mathcal{E} = \{(i, j)\}$, where (i, j) means nodes i and j are connected with edge weight $w_{i,j} \in \mathbb{R}$. A *positive* graph means $w_{i,j} \geq 0, \forall (i, j) \in \mathcal{E}$, while a *signed* graph means $w_{i,j}$ can be negative as well. A node i may have self-loop of weight $u_i \in \mathbb{R}$. Denote by \mathbf{W} the *adjacency matrix*, where $W_{i,j} = w_{i,j}$ if $(i, j) \in \mathcal{E}$ and = 0 otherwise, and $W_{i,i} = u_i$. We assume undirected edges, and thus \mathbf{W} is symmetric. Define the diagonal *degree matrix* \mathbf{D} , where

²BQP objective takes a quadratic form $\mathbf{x}^\top \mathbf{Q} \mathbf{x}$, but \mathbf{Q} is not required to be a Laplacian to a similarity graph.

$D_{i,i} = d_i \triangleq \sum_j W_{i,j}$ is the degree of node i . The *combinatorial graph Laplacian matrix* (Ortega et al. 2018) is defined as $\mathbf{L} \triangleq \mathbf{D} - \mathbf{W}$. To account for self-loops, the *generalized graph Laplacian matrix* is $\mathcal{L} \triangleq \mathbf{D} - \mathbf{W} + \text{diag}(\mathbf{W})$. Note that any real symmetric matrix can be interpreted as a generalized graph Laplacian matrix.

The *graph Laplacian regularizer* (GLR) (Pang and Cheung 2017) that quantifies smoothness of signal $\mathbf{x} \in \mathbb{R}^N$ w.r.t. graph specified by \mathcal{L} is

$$\mathbf{x}^\top \mathcal{L} \mathbf{x} = \sum_{(i,j) \in \mathcal{E}} w_{i,j} (x_i - x_j)^2 + \sum_{i \in \mathcal{V}} u_i x_i^2. \quad (3)$$

GLR is also the objective of our graph classification problem.

Iterative GDPA Linearization

Denote by \mathcal{L} a generalized graph Laplacian matrix to a balanced and connected signed graph \mathcal{G} (with or without self-loops). A *balanced* graph has no cycle of odd number of negative edges. By the *Cartwright-Harary Theorem* (CHT) (Cartwright and Harary 1956), a graph is balanced iff nodes can be colored into blue and red, such that positive (negative) edges connect nodes of the same (different) colors.

GDPA (Yang, Cheung, and Hu 2021) states that a similarity transform $\tilde{\mathcal{L}} = \mathbf{S} \mathcal{L} \mathbf{S}^{-1}$, where $\mathbf{S} = \text{diag}(s_1, \dots, s_N)$, $s_i = v_i^{-1}, \forall i$, and \mathbf{v} is the provably strictly non-zero first eigenvector of \mathcal{L} , has all its Gershgorin disc left-ends aligned exactly at smallest eigenvalue $\lambda_{\min}(\mathcal{L})$, i.e.,

$$\begin{aligned} \tilde{\mathcal{L}}_{i,i} - \sum_{j \neq i} |\tilde{\mathcal{L}}_{i,j}| &= \mathcal{L}_{i,i} - \sum_{j \neq i} |s_i \mathcal{L}_{i,j} / s_j| \\ &= \lambda_{\min}(\mathcal{L}), \quad \forall i \in \{1, \dots, N\}. \end{aligned} \quad (4)$$

To solve an optimization of the form $\min_{\mathcal{L} \succeq 0} Q(\mathcal{L})$, one can leverage GDPA and optimize iteratively as follows. At iteration t with previously computed solution \mathcal{L}^t , compute first eigenvector \mathbf{v}^t to \mathcal{L}^t corresponding to $\lambda_{\min}(\mathcal{L}^t)$; extreme eigenvector \mathbf{v}^t can be computed in linear-time complexity $\mathcal{O}(N)$ using *Locally Optimal Block Preconditioned Conjugate Gradient* (LOBPCG) (Knyazev 2001) assuming a sparse matrix³. Define scalars $s_i^t = 1/v_i^t, \forall i$, then solve

$$\begin{aligned} \min_{\mathcal{L}} Q(\mathcal{L}), \\ \text{s.t. } \mathcal{L}_{i,i} - \sum_{j \neq i} |s_i^t \mathcal{L}_{i,j} / s_j^t| \geq 0, \quad \forall i \in \{1, \dots, N\}. \end{aligned} \quad (5)$$

Linear constraints in (5) ensure that the similarity transform $\tilde{\mathcal{L}} = \mathbf{S} \mathcal{L} \mathbf{S}^{-1}$ is PSD by GCT, and hence solution \mathcal{L} is PSD. Since scalars $\{s_i^t\}$ are computed from first eigenvector \mathbf{v}^t of $\mathcal{L}^t \succeq 0$, by GDPA, similarity transform $\mathbf{S} \mathcal{L}^t \mathbf{S}^{-1}$ has all its disc left-ends aligned exactly at $\lambda_{\min}(\mathcal{L}^t) \geq 0$, and hence \mathcal{L}^t remains feasible at iteration t . Thus, objective $Q(\mathcal{L}^t)$ is monotonically non-increasing with t , and the algorithm converges to a local minimum⁴. We invoke this iterative procedure to solve our posed SDR dual in the sequel.

³For computation reasons, Laplacian \mathcal{L} is typically sparse to specify a sparse graph \mathcal{G} in the GSP literature (Ortega et al. 2018).

⁴See the supplement for an exposition of local convergence.

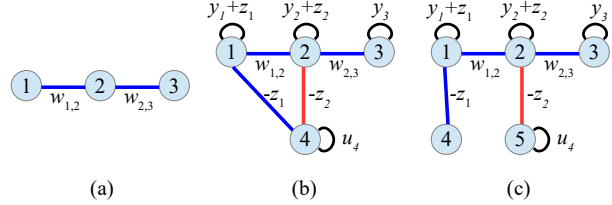


Figure 2: (a) 3-node line graph example. (b) Solution \mathbf{H} to SDR dual (12) as graph Laplacian matrix. (c) Solution $\bar{\mathbf{H}}$ to modified SDR dual (21) as graph Laplacian matrix. Positive / negative edges are colored in blue / red. Self-loop weight u_4 in (b) for node 4 is $u_4 = y_4 + z_1 + z_2$.

Binary Graph Classification

We first formulate the binary graph classification problem and relax it to an SDR problem. We then present its SDR dual with dual variable matrix \mathbf{H} . Finally, we interpret \mathbf{H} as a graph Laplacian, and augment its corresponding graph \mathcal{G} to a balanced graph $\bar{\mathcal{G}}$ for GDPA linearization.

SDR Primal

Given a PSD graph Laplacian matrix $\mathbf{L} \in \mathbb{R}^{N \times N}$ of a positive similarity graph \mathcal{G}^o , one can formulate a binary graph classification problem as

$$\min_{\mathbf{x}} \mathbf{x}^\top \mathbf{L} \mathbf{x}, \quad \text{s.t. } \begin{cases} x_i^2 = 1, \forall i \in \{1, \dots, N\} \\ x_i = \hat{x}_i, \forall i \in \{1, \dots, M\} \end{cases} \quad (6)$$

where $\{\hat{x}_i\}_{i=1}^M$ are the M known labels. The objective in (6) dictates that signal \mathbf{x} is smooth w.r.t. graph \mathcal{G}^o specified by \mathbf{L} . Because \mathbf{L} is PSD (Cheung et al. 2018a), the objective is lower-bounded by 0, i.e., $\mathbf{x}^\top \mathbf{L} \mathbf{x} \geq 0, \forall \mathbf{x} \in \mathbb{R}^N$. The first binary constraint ensures $x_i \in \{-1, 1\}$. The second constraint ensures that entries x_i in signal \mathbf{x} agree with known labels $\{\hat{x}_i\}_{i=1}^M$.

As an example, consider a 3-node line graph shown in Fig. 2(a), where edges (1, 2) and (2, 3) have weights $w_{1,2}$ and $w_{2,3}$, respectively. The corresponding adjacency matrix \mathbf{W} and graph Laplacian matrix \mathbf{L} are

$$\begin{aligned} \mathbf{W} &= \begin{bmatrix} 0 & w_{1,2} & 0 \\ w_{1,2} & 0 & w_{2,3} \\ 0 & w_{2,3} & 0 \end{bmatrix}, \\ \mathbf{L} &= \begin{bmatrix} w_{1,2} & -w_{1,2} & 0 \\ -w_{1,2} & w_{1,2} + w_{2,3} & -w_{2,3} \\ 0 & -w_{2,3} & w_{2,3} \end{bmatrix}. \end{aligned} \quad (7)$$

Suppose known labels are $\hat{x}_1 = 1$ and $\hat{x}_2 = -1$.

(6) is NP-hard (Luo et al. 2010). One can derive a corresponding SDR (Luo et al. 2010) as follows. Define first $\mathbf{X} = \mathbf{x} \mathbf{x}^\top$ and $\mathbf{M} = [\mathbf{X} \ \mathbf{x}; \ \mathbf{x}^\top \ 1]$. \mathbf{M} is PSD because: i) sub-block 1 is trivially PSD, and ii) the *Schur complement* of sub-block 1 of \mathbf{M} is $\mathbf{X} - \mathbf{x} \mathbf{x}^\top = \mathbf{0}$, which is also PSD. Thus, $\mathbf{X} = \mathbf{x} \mathbf{x}^\top$ (or equivalently $\text{rank}(\mathbf{X}) = 1$) implies $\mathbf{M} \succeq 0$, but not vice versa. $\mathbf{X} = \mathbf{x} \mathbf{x}^\top$ and $X_{ii} = 1, \forall i$ imply $x_i^2 = 1, \forall i$. To convexify the problem, we relax $\mathbf{X} = \mathbf{x} \mathbf{x}^\top$ to

$\mathbf{M} \succeq 0$ and write the SDR for optimization variable \mathbf{M} as

$$\min_{\mathbf{x}, \mathbf{X}} \text{Tr}(\mathbf{L}\mathbf{X}) \text{ s.t. } \begin{cases} \mathbf{M} \triangleq \begin{bmatrix} \mathbf{X} & \mathbf{x} \\ \mathbf{x}^\top & 1 \end{bmatrix} \succeq 0 \\ X_{ii} = 1, i \in \{M+1, \dots, N\} \\ x_i = \hat{x}_i, i \in \{1, \dots, M\} \end{cases} \quad (8)$$

where $\text{Tr}(\mathbf{x}^\top \mathbf{L}\mathbf{x}) = \text{Tr}(\mathbf{L}\mathbf{x}\mathbf{x}^\top) = \text{Tr}(\mathbf{L}\mathbf{X})$. Because (8) has linear objective and constraints with an additional PSD cone constraint, $\mathbf{M} \succeq 0$, it is an SDP problem (Gartner and Matousek 2012). We call (8) the *SDR primal*.

Continuing our example, consider ground-truth labels $\mathbf{x} = [1 \ -1 \ 1]^\top$ for the 3-node graph in Fig. 2(a). The corresponding solution matrix $\mathbf{M} = [\mathbf{x}\mathbf{x}^\top \ \mathbf{x}; \ \mathbf{x}^\top \ 1]$ is

$$\mathbf{M} = \begin{bmatrix} 1 & -1 & 1 & 1 \\ -1 & 1 & -1 & -1 \\ 1 & -1 & 1 & 1 \\ 1 & -1 & 1 & 1 \end{bmatrix}. \quad (9)$$

Observe that \mathbf{M} is not a graph Laplacian matrix corresponding to a balanced signed graph, as required by GDPA. This motivates us to investigate the corresponding SDP dual.

SDR Dual

We write the corresponding dual problem based on SDP duality theory (Gartner and Matousek 2012). We first define

$$\mathbf{A}_i = \text{diag}(\mathbf{e}_{N+1}(i)), \quad \mathbf{B}_i = \begin{bmatrix} \mathbf{0}_{N \times N} & \mathbf{e}_N(i) \\ \mathbf{e}_N^\top(i) & 0 \end{bmatrix} \quad (10)$$

where $\mathbf{e}_N(i) \in \{0, 1\}^N$ is a length- N binary *canonical vector* with a single non-zero entry equals to 1 at the i -th entry, $\mathbf{0}_{N \times N}$ is a N -by- N matrix of zeros, and $\text{diag}(\mathbf{v})$ is a diagonal matrix with diagonal entries equal to \mathbf{v} . Note that both \mathbf{A}_i and \mathbf{B}_i are symmetric.

Next, we collect M known labels $\{\hat{x}_i\}_{i=1}^M$ into a vector $\mathbf{b} \in \mathbb{R}^M$ of length M , *i.e.*,

$$b_i = 2\hat{x}_i, \quad \forall i \in \{1, \dots, M\}. \quad (11)$$

We now define the SDR dual of (8) as

$$\begin{aligned} \min_{\mathbf{y}, \mathbf{z}} \quad & \mathbf{1}_{N+1}^\top \mathbf{y} + \mathbf{b}^\top \mathbf{z}, \\ \text{s.t.} \quad & \mathbf{H} \triangleq \sum_{i=1}^{N+1} y_i \mathbf{A}_i + \sum_{i=1}^M z_i \mathbf{B}_i + \begin{bmatrix} \mathbf{L} & \mathbf{0}_N \\ \mathbf{0}_N^\top & 0 \end{bmatrix} \succeq 0 \end{aligned} \quad (12)$$

where $\mathbf{1}_N$ is a length- N vector of ones, and dual variables are $\mathbf{y} \in \mathbb{R}^{N+1}$ and $\mathbf{z} \in \mathbb{R}^M$. Given that (12) is a minimization, when $b_i < 0$ (*i.e.*, $\hat{x}_i < 0$), the corresponding z_i is non-negative⁵, *i.e.*, $z_i \geq 0$. Similarly, for $b_i > 0$, $z_i \leq 0$. Thus, the signs of z_i 's are known *a priori*. Without loss of generality, we assume $z_i \leq 0, \forall i \in \{1, \dots, M_1\}$ and $z_i \geq 0, \forall i \in \{M_1+1, \dots, M\}$, where $1 \leq M_1 < M$, in the sequel.

⁵ $z_i < 0$ when $b_i < 0$ would mean a worse objective and larger Gershgorin disc radii for rows i and $N+1$ of matrix \mathbf{H} , making \mathbf{H} more difficult to reside in the PSD cone $\mathbf{H} \succeq 0$.

Reformulating the SDR Dual

We interpret $\mathbf{H} \in \mathbb{R}^{(N+1) \times (N+1)}$ in (12) as a graph Laplacian corresponding to a signed graph \mathcal{G} . However, \mathcal{G} is *not balanced*, because of the last row / column in \mathbf{H} . To see this, we write

$$\mathbf{H} = \begin{bmatrix} \mathcal{L}_y & \mathbf{g} \\ \mathbf{g}^\top & y_{N+1} \end{bmatrix} \quad (13)$$

where $\mathbf{g} = [z_1 \dots z_M \ \mathbf{0}_{N-M}^\top]^\top$. Matrix $\mathcal{L}_y \in \mathbb{R}^{N \times N}$, defined as $\mathcal{L}_y \triangleq \text{diag}(y_1, \dots, y_N) + \mathbf{L}$, is a generalized Laplacian to a N -node positive graph \mathcal{G}^+ . However, node $N+1$ has *both* positive *and* negative edges to \mathcal{G}^+ stemming from negative z_i 's and positive z_i 's, respectively. As a result, \mathbf{H} is not a Laplacian to a balanced signed graph.

Continuing our 3-node line graph example with Laplacian \mathbf{L} , the corresponding \mathcal{L}_y and \mathbf{H} are

$$\begin{aligned} \mathcal{L}_y &= \begin{bmatrix} y_1 + w_{1,2} & -w_{1,2} & 0 \\ -w_{1,2} & y_2 + w_{1,2} + w_{2,3} & -w_{2,3} \\ 0 & -w_{2,3} & y_3 + w_{2,3} \end{bmatrix}, \\ \mathbf{H} &= \begin{bmatrix} y_1 + w_{1,2} & -w_{1,2} & 0 & z_1 \\ -w_{1,2} & y_2 + w_{1,2} + w_{2,3} & -w_{2,3} & z_2 \\ 0 & -w_{2,3} & y_3 + w_{2,3} & 0 \\ z_1 & z_2 & 0 & y_4 \end{bmatrix}. \end{aligned} \quad (14)$$

Interpreting \mathbf{H} as a graph Laplacian, node 1 has degree $d_1 = y_1 + w_{1,2} = u_1 + w_{1,2} - z_1$, and thus $u_1 = y_1 + z_1$. Similarly, node 4 has degree $d_4 = y_4 = u_4 - z_1 - z_2$, and thus $u_4 = y_4 + z_1 + z_2$. See Fig. 2(b) for an illustration of this unbalanced signed graph \mathcal{G} . More generally, self-loop weights are $u_i = y_i + z_i$ for $i \in \{1, \dots, M\}$, $u_i = y_i$ for $i \in \{M+1, \dots, N\}$, and $u_{N+1} = y_{N+1} + \sum_{j=1}^M z_j$.

Node $N+1$ has positive and negative edges, with respective weights $\{-z_i\}_{i=1}^{M_1}$ and $\{-z_i\}_{i=M_1+1}^M$ to \mathcal{G}^+ , and a self-loop with weight u_{N+1} . We construct an *augmented* graph $\bar{\mathcal{G}}$ with $N+2$ nodes from \mathcal{G} by splitting node $N+1$ in \mathcal{G} into two in $\bar{\mathcal{G}}$, assigning positive and negative edges to the two respectively. The graph construction procedure is

1. Construct each i of first N nodes with the same inter-node edges as \mathcal{G}^+ plus self-loop with weight u_i .
2. Construct node $N+1$ with positive edges $\{-z_i\}_{i=1}^{M_1}$, and node $N+2$ with negative edges $\{-z_i\}_{i=M_1+1}^M$, to the first N nodes in sub-graph \mathcal{G}^+ .
3. Add self-loop for nodes $N+2$ with weight u_{N+1} .

Step 3 implies that nodes $N+1$ and $N+2$ have degrees $\kappa_{N+1} \triangleq -\sum_{i=1}^{M_1} z_i$ and $\kappa_{N+2} \triangleq u_{N+1} - \sum_{i=M_1+1}^M z_i$, respectively. Denote by $\bar{\mathbf{H}} \in \mathbb{R}^{(N+2) \times (N+2)}$ the graph Laplacian matrix corresponding to $\bar{\mathcal{G}}$. Continuing our 3-node graph example, Fig. 2(c) shows the augmented graph $\bar{\mathcal{G}}$, and the corresponding Laplacian $\bar{\mathbf{H}}$ is

$$\bar{\mathbf{H}} = \begin{bmatrix} d_1 & -w_{1,2} & 0 & z_1 & 0 \\ -w_{1,2} & d_2 & -w_{2,3} & 0 & z_2 \\ 0 & -w_{2,3} & d_3 & 0 & 0 \\ z_1 & 0 & 0 & -z_1 & 0 \\ 0 & z_2 & 0 & 0 & u_4 - z_2 \end{bmatrix} \quad (15)$$

where $d_i = y_i + \sum_{j \neq i} w_{i,j}$ is the degree of node i for $i \in \{1, \dots, N\}$.

Crucially, $\bar{\mathbf{H}}$ and \mathbf{H} are related in spectral terms by the following important lemma.

Lemma 1. *Smallest eigenvalue $\lambda_{\min}(\bar{\mathbf{H}})$ of graph Laplacian $\bar{\mathbf{H}}$ to augmented graph $\tilde{\mathcal{G}}$ is a lower bound for smallest eigenvalue $\lambda_{\min}(\mathbf{H})$ of Laplacian \mathbf{H} to \mathcal{G} , i.e.,*

$$\lambda_{\min}(\bar{\mathbf{H}}) \leq \lambda_{\min}(\mathbf{H}). \quad (16)$$

Proof. Denote by \mathcal{G} the graph represented by generalized graph Laplacian \mathbf{H} , with inter-node edge weights $\{w_{i,j}\}$ and self-loop weights $\{u_i\}$. Denote by $\mathbf{v} \in \mathbb{R}^{N+1}$ the first eigenvector of \mathbf{H} corresponding to the smallest eigenvalue $\lambda_{\min}(\mathbf{H})$. From (3), GLR of \mathbf{H} computed using \mathbf{v} is

$$\begin{aligned} \mathbf{v}^\top \mathbf{H} \mathbf{v} &= \sum_{(i,j) \in \mathcal{E} \mid 1 \leq i,j \leq N} w_{i,j} (v_i - v_j)^2 - \sum_{i=1}^M z_i (v_{N+1} - v_i)^2 \\ &\quad + \sum_{i=1}^N u_i v_i^2 + u_{N+1} v_{N+1}^2. \end{aligned} \quad (17)$$

Now construct length- $(N+2)$ vector $\boldsymbol{\alpha} \in \mathbb{R}^{N+2}$, where $\boldsymbol{\alpha} = [v_1 \dots v_N \ v_{N+1} \ v_{N+1}]^\top$. GLR of $\bar{\mathbf{H}}$ using $\boldsymbol{\alpha}$ is

$$\begin{aligned} \boldsymbol{\alpha}^\top \bar{\mathbf{H}} \boldsymbol{\alpha} &= \sum_{(i,j) \in \mathcal{E} \mid 1 \leq i,j \leq N} w_{i,j} (v_i - v_j)^2 - \sum_{i=1}^{M_1} z_i (v_{N+1} - v_i)^2 \\ &\quad - \sum_{i=M_1+1}^M z_i (v_{N+1} - v_i)^2 + \sum_{i=1}^N u_i v_i^2 + u_{N+1} v_{N+1}^2. \end{aligned} \quad (18)$$

Thus, $\mathbf{v}^\top \mathbf{H} \mathbf{v} = \boldsymbol{\alpha}^\top \bar{\mathbf{H}} \boldsymbol{\alpha}$. Since first eigenvector \mathbf{v} of \mathbf{H} minimizes its Rayleigh quotient,

$$\lambda_{\min}(\mathbf{H}) = \frac{\mathbf{v}^\top \mathbf{H} \mathbf{v}}{\mathbf{v}^\top \mathbf{v}} \stackrel{(a)}{\geq} \frac{\boldsymbol{\alpha}^\top \bar{\mathbf{H}} \boldsymbol{\alpha}}{\boldsymbol{\alpha}^\top \boldsymbol{\alpha}} \stackrel{(b)}{\geq} \lambda_{\min}(\bar{\mathbf{H}}). \quad (19)$$

(a) holds since $\mathbf{v}^\top \mathbf{v} \leq \boldsymbol{\alpha}^\top \boldsymbol{\alpha}$ by construction, and (b) holds since $\lambda_{\min}(\bar{\mathbf{H}}) = \min_{\mathbf{x}} \frac{\mathbf{x}^\top \bar{\mathbf{H}} \mathbf{x}}{\mathbf{x}^\top \mathbf{x}}$. \square

In our experiments, we verify numerically that the bound $\lambda_{\min}(\bar{\mathbf{H}}) \leq \lambda_{\min}(\mathbf{H})$ was tight in realistic datasets.

Given Lemma 1, we reformulate the SDR dual (12) by keeping the same objective but imposing the PSD cone constraint on $\bar{\mathbf{H}}$ instead of \mathbf{H} . First, define \mathbf{A}'_i , \mathbf{B}'_i and \mathbf{B}''_i similarly to (10) but for a larger $(N+2)$ -by- $(N+2)$ matrix; i.e., $\mathbf{A}'_i \triangleq \text{diag}(\mathbf{e}_{N+2}(i))$,

$$\mathbf{B}'_i \triangleq \begin{bmatrix} \mathbf{B}_i & \mathbf{0}_{N+1} \\ \mathbf{0}_{N+1}^\top & 0 \end{bmatrix}, \quad \mathbf{B}''_i \triangleq \begin{bmatrix} \mathbf{0}_{(N+1) \times (N+1)} & \mathbf{e}_{N+1}(i) \\ \mathbf{e}_{N+1}^\top(i) & 0 \end{bmatrix}. \quad (20)$$

The reformulated SDR dual is

$$\begin{aligned} \min_{\mathbf{y}, \mathbf{z}} \quad & \mathbf{1}_{N+1}^\top \mathbf{y} + \mathbf{b}^\top \mathbf{z}, \\ \text{s.t.} \quad & \bar{\mathbf{H}} \triangleq \sum_{i=1}^N y_i \mathbf{A}'_i + \kappa_{N+1} \mathbf{A}'_{N+1} + \kappa_{N+2} \mathbf{A}'_{N+2} \\ & + \sum_{i=1}^{M_1} z_i \mathbf{B}'_i + \sum_{i=M_1+1}^M z_i \mathbf{B}''_i + \begin{bmatrix} \mathbf{L} & \mathbf{0}_{N \times 2} \\ \mathbf{0}_{2 \times N} & \mathbf{0}_{2 \times 2} \end{bmatrix} \succeq 0 \end{aligned} \quad (21)$$

where κ_{N+1} and κ_{N+2} are the degrees of nodes $N+1$ and $N+2$, respectively, defined earlier.

We can bound the difference in objective values between the optimal solutions to (12) and (21) as follows. We first construct yet another modified graph $\tilde{\mathcal{G}}$ from \mathcal{G} , where weight $-z_i$ of each edge from node $N+1$ to node $i \in \{1, \dots, M\}$ is incremented by ϕ . This results in another related graph Laplacian matrix $\tilde{\mathbf{H}}$ for modified $\tilde{\mathcal{G}}$. Continuing our example, the modified graph Laplacian $\tilde{\mathbf{H}}$ from \mathbf{H} in (14) is

$$\tilde{\mathbf{H}} = \mathbf{H} + \begin{bmatrix} \phi & 0 & 0 & -\phi \\ 0 & \phi & 0 & -\phi \\ 0 & 0 & 0 & 0 \\ -\phi & -\phi & 0 & 2\phi \end{bmatrix}. \quad (22)$$

Similar to Lemma 1, we claim in the following lemma that $\bar{\mathbf{H}}$ and \mathbf{H} are related in spectral terms.

Lemma 2. *The smallest eigenvalue $\lambda_{\min}(\mathbf{H})$ of graph Laplacian \mathbf{H} to graph \mathcal{G} is a lower bound for $\lambda_{\min}(\tilde{\mathbf{H}})$ of Laplacian $\tilde{\mathbf{H}}$ to $\tilde{\mathcal{G}}$, i.e.,*

$$\lambda_{\min}(\mathbf{H}) \leq \lambda_{\min}(\tilde{\mathbf{H}}). \quad (23)$$

See the proof in the supplementary file. The corollary is that $\tilde{\mathbf{H}} \succeq 0$ if $\mathbf{H} \succeq 0$, or more simply, $\tilde{\mathbf{H}} \succeq \mathbf{H}$. This means that minimizing the same objective in (12) but using the more relaxed constraint $\tilde{\mathbf{H}} \succeq 0$ instead will yield an objective value $F(\tilde{\mathbf{H}})$ that is no worse than $F(\mathbf{H})$. Given $\tilde{\mathbf{H}} \succeq \mathbf{H} \succeq \bar{\mathbf{H}}$, we know $F(\tilde{\mathbf{H}}) \leq F(\mathbf{H}) \leq F(\bar{\mathbf{H}})$. Thus, we can bound the approximation error $|F(\bar{\mathbf{H}}) - F(\mathbf{H})|$ between the modified SDR dual (21) and the original SDR dual (12) as

$$|F(\bar{\mathbf{H}}) - F(\mathbf{H})| \leq |F(\bar{\mathbf{H}}) - F(\tilde{\mathbf{H}})|. \quad (24)$$

Finally, we note that minimizing objective in (12) with constraint $\tilde{\mathbf{H}} \geq 0$ is much easier if ϕ is sufficiently large such that all edges from node $N+1$ becomes positive. In such case, $\tilde{\mathcal{G}}$ is a positive graph, and GDPA linearization can be applied. Thus, the error bound (24) can be numerically computed efficiently for each instant of SDR dual (12).

Given $\bar{\mathbf{H}}$ is a Laplacian to a balanced graph, we discuss using GDPA linearization to solve (21) next.

Algorithm Implementation

GDPA Linearization

We replace the PSD cone constraint on $\bar{\mathbf{H}}$ in (21) with $N+2$ linear constraints via GDPA. Specifically, at iteration t , we compute first eigenvector \mathbf{v}^t of solution $\bar{\mathbf{H}}^t$

using LOBPCG (Knyazev 2001). We define scalars $s_i = 1/v_i^t, \forall i \in \{1, \dots, N+2\}$. Finally, we write $N+2$ constraints corresponding to $\lambda_{\min}^-(\mathbf{S}^T \mathbf{H} \mathbf{S}^{-1}) \geq 0$, where $\mathbf{S} = \text{diag}(s_1, \dots, s_{N+2})$, *i.e.*,

$$\bar{H}_{i,i} - \sum_{j \neq i} |s_i \bar{H}_{i,j} / s_j| \geq 0, \quad \forall i \in \{1, \dots, N+2\}. \quad (25)$$

Note that the absolute value operation can be appropriately removed for each term $s_i \bar{H}_{i,j} / s_j$, since the signs for s_i and $\bar{H}_{i,j}$ are known. Together with linear objective in (21), this constitutes an LP for variables \mathbf{y} and \mathbf{z} , solvable using an available fast LP solver (Vanderbei 2021)⁶. Compared to SDR primal (8) with a large matrix variable $\mathbf{M} \in \mathbb{R}^{(N+1) \times (N+1)}$, dimensions of our LP variables, $\mathbf{y} \in \mathbb{R}^{N+1}$ and $\mathbf{z} \in \mathbb{R}^M$, are much smaller.

A sequence of LPs are solved, each time with scalars s_i 's updated from computed solution $\bar{\mathbf{H}}^t$, until convergence. The bulk of the complexity resides in the computation of the first eigenvector \mathbf{v}^t for each LP solution $\bar{\mathbf{H}}^t$. LOBPCG (Knyazev 2001) is an iterative algorithm running in linear time for extreme eigenvectors of sparse matrices, which further benefits from *warm start*: with a good initial guess for \mathbf{v}^t , the algorithm converges faster. Since $\bar{\mathbf{H}}^t$ changes gradually during the iterations, we use previously computed eigenvector \mathbf{v}^{t-1} of $\bar{\mathbf{H}}^{t-1}$ as initial guess for \mathbf{v}^t of $\bar{\mathbf{H}}^t$. Experiments show that warm start improves convergence speed significantly.

Initialization & Prediction Label Extraction

Our posed LP requires an initial $\bar{\mathbf{H}}^0$ to compute first eigenvector \mathbf{v}^0 , so that scalars $\{s_i\}_{i=1}^{N+2}$ can be defined for $N+2$ linear constraints in (25). To initialize $\bar{\mathbf{H}}^0$, we set $\mathbf{y}^0 = [\mathbf{1}_M^\top \mathbf{0}_{N-M}^\top M]^\top$ and $\mathbf{z}^0 = [-\hat{x}_1 \dots -\hat{x}_M]$. $\bar{\mathbf{H}}^0$ can then be computed using definition of $\bar{\mathbf{H}}$ in (21).

As similarly done in (Luo et al. 2010), we extract labels $\mathbf{x}^* = [x_1 \dots x_N]^\top$ from converged LP solution \mathbf{y}^* and \mathbf{z}^* as follows. We first construct \mathbf{H}^* using \mathbf{y}^* and \mathbf{z}^* using definition of \mathbf{H} in (12). We then compute $\mathbf{x}^* = \text{sign}(\hat{x}_1 v_1 \mathbf{v})$, where v_1 is the first entry of the first eigenvector \mathbf{v} of \mathbf{H}^* . See (Luo et al. 2010) for details of recovering SDP primal variables from dual variables in BQP. Finally, we extract the prediction labels as $\tilde{\mathbf{x}} = [x_{M+1}^*, \dots, x_N^*]^\top$.

Experiments

Experimental Setup

We implemented our GDPA classifier in Matlab⁷, and evaluated it in terms of average classification error rate and running time. All computations were carried out on a Windows 10 64bit PC with AMD Ryzen Threadripper 3960X 24-core processor 3.80 GHz and 128GB of RAM. We compared our algorithm against the following schemes that solve the SDR primal problem (8) directly: i) two primal-dual interior-point solvers for SDP, SeDuMi and MOSEK (CVX 2020), ii) an

⁶The lowest complexity of a general LP solver (Jiang et al. 2020) to date is $\mathcal{O}(N^{2.055})$. Note that the LP field is still fast-evolving, and our proposal is not tied to a specific LP solver.

⁷available at https://anonymous.4open.science/r/gc_-80C0

ADMM first-order operator-splitting solver CDCS (Zheng, Fantuzzi, and Papachristodoulou 2019; CDCS 2016), iii) a spectrahedron-based relaxation solver SDCut (Wang, Shen, and van den Hengel 2013; SDCut 2013) that involves LBFGS-B (Zhu et al. 1997), and iv) a biconvex relaxation solver BCR (Shah et al. 2016; BCR 2020), all of which are implemented in Matlab. Further, we employed CDCS again to solve our modified SDR dual problem (21). We focus our comparison with SDR schemes because, again, SDR is known to provide good error-bounded approximations in general for NP-hard QCQP problems (Luo et al. 2010).

In addition, we compared against the following non-SDR methods approximating original classifier formulation (6) directly. A recent method called *stochastic neighborhood search* (SNS) (Lam and Liew 2020; SNS 2021) solves (6) by alternately applying Karush–Kuhn–Tucker optimality condition guided deterministic search and bootstrapping sampling based stochastic search. We solved a relaxed version of (6) using SeDuMi, where constraint $x_i^2 = 1$ was relaxed to a box constraint $x_i \in [-1, 1]$ —we denote this method by GLR-box. Finally, binary constraint $x_i^2 = 1$ can be ignored entirely, and objective $\mathbf{x}^\top \mathbf{L} \mathbf{x}$ in (6) can be optimized simply by computing extreme eigenvectors plus rounding. We denote this class of spectral methods by SPEC, which are fast but are known to have poor worst-case errors (Guattery and Miller 1998).

Experimental Results

We first show in Table 1 that SPEC has by far the worst performance in binary signal restoration compared to SDR-based schemes and SNS, demonstrating the limitations of spectral methods in general. Specifically, following an illustrative example in (Lam and Liew 2020), we first corrupted a length- N 1-D signal $[\mathbf{1}_{N/2}^\top, -\mathbf{1}_{N/2}^\top]$ with iid noise, then solved the optimization $\max_{x_i \in \{-1, 1\}} \mathbf{x}^\top \mathbf{P} \mathbf{x}$, where $\mathbf{P} = [\mathbf{1} \ \mathbf{c}^\top; \mathbf{c} \ \mathbf{W}]$. Here, \mathbf{c} denotes the noisy 1-D signal, and \mathbf{W} denotes the adjacency matrix corresponding to an unweighted line graph. We optimized the above objective using SPEC, SDR primal formulation like (8), our proposed GDPA, and SNS. Results were averaged over 100 runs. Table 1 shows that SPEC performed by far the worst at all problem sizes ($N = 100$ or 200), types of line graphs (1-hop or 2-hop neighbor) and noise standard deviation σ . In contrast, GDPA performed similarly to SDR primal and non-SDR scheme SNS. We thus remove SPEC from experimental comparisons in the sequel.

We next evaluate competing schemes on classification error and runtime on real datasets. For each dataset, we first performed *min-max* (Russell and Norvig 2009) and *standardization* (Dong et al. 2020), two different data re-scaling schemes, to the features of dataset samples, used to compute graph edge weights via an exponential kernel (Ortega et al. 2018). For experimental efficiency, we performed a K -fold ($K \leq 5$) split for each dataset with random seed 0, and then created 10 instances of 50% training–50% test split for each fold, with random seeds 1–10 (Russell and Norvig 2009). We used 50% training–50% test split for each experiment. See the supplementary file for detailed experimental settings. Table 2 and Fig. 3 (left) show average classification error rates and runtime (in log scale) of 17 binary datasets (UCI 2021; Lib-

Table 1: Binary signal restoration error (%). Original signal $[1_{N/2}^\top, -1_{N/2}^\top]$ is firstly corrupted using white noise with std σ and then restored using spectral method SPEC, SDP solver SeDuMi on SDR primal in (8), proposed GDPA and non-SDR method SNS. Results are averaged over 100 runs.

| N | graph | 1-hop neighbor | | | 2-hop neighbor | | |
|-----|-------------|----------------|-------|-------|----------------|-------|-------|
| | | σ | 1 | 1.5 | 2 | 1 | 1.5 |
| 100 | SPEC | 13.04 | 23.24 | 29.59 | 10.02 | 20.94 | 28.06 |
| | SDR primal | 2.45 | 11.96 | 20.82 | 0.90 | 4.82 | 12.92 |
| | GDPA | 2.78 | 11.01 | 19.57 | 0.86 | 3.57 | 9.13 |
| | SNS | 1.97 | 11.01 | 19.88 | 0.63 | 2.50 | 8.32 |
| 200 | SPEC | 13.54 | 23.38 | 29.36 | 11.19 | 21.69 | 28.20 |
| | SDR primal | 1.76 | 10.78 | 19.16 | 0.28 | 3.01 | 10.87 |
| | GDPA | 2.46 | 10.81 | 18.67 | 0.39 | 2.83 | 8.52 |
| | SNS | 1.72 | 10.92 | 19.09 | 0.20 | 1.48 | 7.36 |

Table 2: Mean classification error (%) of 17 binary datasets.

| data re-scaling | min-max | standardization |
|-----------------|---------|-----------------|
| SeDuMi (8) | 30.19 | 32.60 |
| MOSEK (8) | 30.31 | 32.61 |
| CDCS (8) | 30.76 | 31.76 |
| CDCS (21) | 30.08 | 29.40 |
| BCR | 27.60 | 26.24 |
| SDcut | 27.49 | 26.81 |
| GLR-box | 28.63 | 28.38 |
| SNS | 33.75 | 30.50 |
| GDPA | 28.21 | 26.94 |

SVM 2021) with problem sizes from 29 to 400, respectively. The x -axis of each plot denotes the datasets in ascending order of problem sizes. Fig. 3 (right) shows runtime using the same dataset `cod-rna` with problem sizes from 4 to 24428. We did not execute SeDuMi (8), MOSEK (8), CDCS (8), CDCS (21), BCR, SDcut or GLR-box when problem size exceeded 976.

In terms of classification error rate, CDCS solving the modified dual (21) had similar performance as the original SDR primal (SeDuMi (8), MOSEK (8) and CDCS (8)), showing the validity of our proposed modified SDR dual (21). Further, our proposed GDPA closely approximated the modified SDR dual (CDCS (21)) in performance, demonstrating the effectiveness of our projection-free GDPA linearization scheme. By factorizing a PSD matrix $\mathbf{M} = \mathbf{X}\mathbf{X}^\top$, BCR avoided tuning of any forward progress step size after each PSD cone projection, which may explain its slightly better average performance. However, BCR solved a non-convex optimization problem converging to a local minimum, and thus occasionally the performance was relatively poor (*e.g.*, see `colon-cancer` in the error rate plots in the supplementary file). Overall, all solvers performed similarly given constructed similarity graphs in the two cases.

In terms of runtime, BCR was competitive with GDPA when the problem size was small, but *GDPA significantly outperformed all competing solvers when the problem size was large*. Specifically, the speed gain increased as problem size increased; for `madelon` with size 400, the speedup of GDPA over the next fastest scheme SNS was 34 \times .

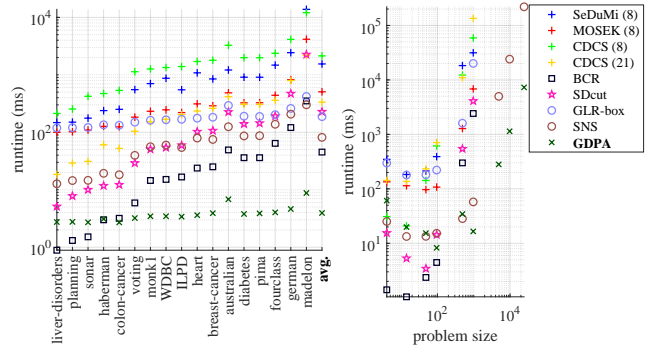


Figure 3: Runtime (ms) on 17 datasets (left) with problem sizes 29 to 400 and `cod-rna` (right) with problem sizes 4 to 24428.

Fig. 3 (right) shows that the computation time for GDPA increased gracefully as the problem size increased to very large sizes. One reason for our dramatic speed gain is the fast computation of first eigenvectors using LOBPCG, which benefited from warm start. In general, GDPA performed fewer than 10 LP’s until convergence. In contrast, both CDCS and SDcut required full matrix eigen-decomposition of a matrix of size $N \times N$ per iteration; the speedup of replacing the full eigen-decomposition with one LP plus first eigenvector computation per iteration was significant. For BCR, each iteration required either N -dimensional matrix inversion for a least-squares problem or iterative gradient descent, which was computationally expensive as the problem size increased. SNS required many matrix-vector multiplications—which was time-consuming as the problem size increased—though manually adjusting the number of neighborhood vectors can potentially improve speed. On average, GDPA enjoyed a 28 \times speedup over the next fastest solver SNS.

On average, the difference between $\lambda_{\min}(\mathbf{H})$ and $\lambda_{\min}(\bar{\mathbf{H}})$ in Lemma 1 is 1.1608×10^{-7} , which is very small. This demonstrates the tightness of bound $\lambda_{\min}(\bar{\mathbf{H}}) \leq \lambda_{\min}(\mathbf{H})$ in practice, and thus the effectiveness of Lemma 1.

Conclusion

We propose a fast projection-free algorithm for the binary graph classification problem. The key idea is to replace the difficult positive semi-definite (PSD) cone constraint with linear constraints derived from the recent Gershgorin disc perfect alignment (GDPA) theory, so that each iteration requires only one linear program (LP) and one first eigenvector computation. Experiments show that our algorithm enjoyed on average 28 \times speedup over the next fastest competitor while retaining comparable label prediction performance.

As an optimization problem, binary graph classification is rather narrowly defined (though multi-class classification can be implemented as a tree of binary classifiers). Further, performance depends heavily on the construction of a good similarity graph, which is outside this paper’s scope. However, we conjecture that the general methodology of GDPA linearization can be similarly tailored to other QCQP problems with PSD cone constraints. We anticipate that speedups in other QCQP problems will also be significant.

References

BCR. 2020. BCR implementation. https://github.com/Axeldnahcram/biconvex_relaxation. Accessed: 2022-8-15.

Belkin, M.; Matveeva, I.; and Niyogi, P. 2004. Regularization and semisupervised learning on large graphs. In *Shawe-Taylor J., Singer Y. (eds) Learning Theory, COLT 2004, Lecture Notes in Computer Science*, volume 3120, 624–638.

Bishop, C. M. 2006. *Pattern Recognition and Machine Learning (Information Science and Statistics)*. Berlin, Heidelberg: Springer-Verlag. ISBN 0387310738.

Boyd, S.; Parikh, N.; Chu, E.; Peleato, B.; and Eckstein, J. 2011. Distributed Optimization and Statistical Learning via the Alternating Direction method of Multipliers. In *Foundations and Trends in Optimization*, volume 3, no.1, 1–122.

Cartwright, D.; and Harary, F. 1956. Structural balance: a generalization of Heider's theory. In *Psychological Review*, volume 63, no.5, 277–293.

CDCS. 2016. CDCS implementation. <https://github.com/oxfordcontrol/CDCS>. Accessed: 2022-8-15.

Cheung, G.; Magli, E.; Tanaka, Y.; and Ng, M. 2018a. Graph Spectral Image Processing. In *Proceedings of the IEEE*, volume 106, no.5, 907–930.

Cheung, G.; Su, W.-T.; Mao, Y.; and Lin, C.-W. 2018b. Robust Semisupervised Graph Classifier Learning with Negative Edge Weights. In *IEEE Transactions on Signal and Information Processing over Networks*, volume 4, no.4, 712–726.

Chung, F. 1996. *Spectral Graph Theory*. American Mathematical Society.

CVX. 2020. CVX Research. <http://cvxr.com/cvx/>. Accessed: 2022-8-15.

Dittrich, T.; and Matz, G. 2020. Signal Processing on Signed Graphs: Fundamentals and potentials. In *IEEE Signal Processing Magazine*, volume 37, no.6, 86–98.

Dong, M.; Wang, Y.; Yang, X.; and Xue, J. 2020. Learning Local Metrics and Influential Regions for Classification. *IEEE TPAMI*, 42(6): 1522–1529.

Dong, X.; Thanou, D.; Rabbat, M.; and Frossard, P. 2019. Learning Graphs From Data: A Signal Representation Perspective. *IEEE Signal Processing Magazine*, 36(3): 44–63.

Gartner, B.; and Matousek, J. 2012. *Approximation Algorithms and Semidefinite Programming*. Springer.

Gavish, M.; Nadler, B.; and Coifman, R. 2010. Multiscale wavelets on trees, graphs and high dimensional data: Theory and applications to semi-supervised learning. In *27th International Conference on Machine Learning*. Haifa, Israel.

Goemans, M.; and Williamson, D. 1995. Improved Approximation Algorithms for Maximum Cut and Satisfiability Problems Using Semidefinite Programming. *J. ACM*, 42(6): 1115–1145.

Guattery, S.; and Miller, G. L. 1998. On the Quality of Spectral Separators. *SIAM Journal on Matrix Analysis and Applications*, 19(3): 701–719.

Guillory, A.; and Bilmes, J. 2009. Label Selection on Graphs. In *Twenty-Third Annual Conference on Neural Information Processing Systems*. Vancouver, Canada.

Helmberg, C.; Rendl, F.; Vanderbei, R.; and Wolkowicz, H. 1996. An interior-point method for semidefinite programming. In *SIAM J. Optim.*, volume 6, no.2, 342–361.

Jiang, S.; Song, Z.; Weinstein, O.; and Zhang, H. 2020. Faster Dynamic Matrix Inverse for Faster LPs. *arXiv:2004.07470*.

Knyazev, A. V. 2001. Toward the Optimal Preconditioned Eigensolver: Locally Optimal Block Preconditioned Conjugate Gradient Method. *SIAM Journal on Scientific Computing*, 23(2): 517–541.

Kunegis, J.; Schmidt, S.; Lommatzsch, A.; Lerner, J.; Luca, E. D.; and Albayrak, S. 2010. Spectral analysis of signed graphs for clustering, prediction and visualization. In *SIAM International Conference on Data Mining*. Columbus, OH.

Lam, B. S.; and Liew, A. W. C. 2020. A Fast Binary Quadratic Programming Solver based on Stochastic Neighborhood Search. *IEEE Transactions on Pattern Analysis and Machine Intelligence*, 1–1.

Li, Z.; Liu, J.; and Tang, X. 2008. Pairwise constraint propagation by semidefinite programming for semi-supervised classification. In *ACM International Conference on Machine Learning*. Helsinki, Finland.

LibSVM. 2021. LibSVM Data: Classification (Binary Class). <https://www.csie.ntu.edu.tw/~cjlin/libsvmtools/datasets/binary.html>. Accessed: 2022-8-15.

Luo, Z.; Ma, W.; So, A. M.; Ye, Y.; and Zhang, S. 2010. Semidefinite Relaxation of Quadratic Optimization Problems. *IEEE Signal Processing Magazine*, 27(3): 20–34.

Moutafis, P.; Leng, M.; and Kakadiaris, I. A. 2017. An Overview and Empirical Comparison of Distance Metric Learning Methods. *IEEE Transactions on Cybernetics*, 47(3): 612–625.

O'Donoghue, B.; Chu, E.; Parikh, N.; and Boyd, S. 2016. Conic Optimization via Operator Splitting and Homogeneous Self-Dual Embedding. In *Journal of Optimization Theory and Applications*, volume 169, no.3, 1042–1068.

Ortega, A.; Frossard, P.; Kovacevic, J.; Moura, J. M. F.; and Vandergheynst, P. 2018. Graph Signal Processing: Overview, Challenges, and Applications. In *Proceedings of the IEEE*, volume 106, no.5, 808–828.

Pang, J.; and Cheung, G. 2017. Graph Laplacian Regularization for Inverse Imaging: Analysis in the Continuous Domain. In *IEEE Transactions on Image Processing*, volume 26, no.4, 1770–1785.

Russell, S.; and Norvig, P. 2009. *Artificial Intelligence: A Modern Approach*. USA: Prentice Hall Press, 3rd edition. ISBN 0136042597.

SDcut. 2013. SDcut implementation. <https://github.com/chhshen/SDCut>. Accessed: 2022-8-15.

Shah, S.; Kumar, A.; Castillo, C.; Jacobs, D.; Studer, C.; and Goldstein, T. 2016. Biconvex Relaxation for Semidefinite Programming in Computer Vision. In *European Conference on Computer Vision*. Amsterdam, the Netherlands.

Shuman, D.; Faraji, M.; and Vandergheynst, P. 2011. Semi-supervised learning with spectral graph wavelets. In *International Conference on Sampling Theory and Applications (SampTA)*. Singapore.

SNS. 2021. SNS implementation. <https://github.com/bensonsylam/BQP>. Accessed: 2021-10-10.

UCI. 2021. UCI machine learning repository. <https://archive.ics.uci.edu/ml/datasets.php>. Accessed: 2022-8-15.

Vanderbei, R. 2021. *Linear Programming: Foundations and Extensions (5th Edition)*. Springer Nature.

Varga, R. S. 2004. *Gershgorin and his circles*. Springer.

Wang, P.; Shen, C.; Hengel, A.; and Torr, P. 2017. Large-Scale Binary Quadratic Optimization Using Semidefinite Relaxation and Applications. *IEEE Transactions on Pattern Analysis and Machine Intelligence*, 39(3): 470–485.

Wang, P.; Shen, C.; and van den Hengel, A. 2013. A Fast Semidefinite Approach to Solving Binary Quadratic Problems. In *IEEE International Conference on Computer Vision and Pattern Recognition*. Portland, OR.

Yang, C.; Cheung, G.; and Hu, W. 2021. Signed Graph Metric Learning via Gershgorin Disc Perfect Alignment. *IEEE Transactions on Pattern Analysis and Machine Intelligence*, 1–1.

Zheng, Y.; Fantuzzi, G.; and Papachristodoulou, A. 2019. Fast ADMM for Sum-of-Squares Programs Using Partial Orthogonality. *IEEE Transactions on Automatic Control*, 64(9): 3869–3876.

Zheng, Y.; Fantuzzi, G.; Papachristodoulou, A.; Goulart, P.; and Wynn, A. 2020. Chordal decomposition in operator-splitting methods for sparse semidefinite programs. *Mathematical Programming*, 180: 489—532.

Zhou, D.; Bousquet, O.; Lal, T. N.; Weston, J.; and Scholkopf, B. 2003. Learning with local and global consistency. In *16th International Conference on Neural Information Processing (NIPS)*. Whistler, Canada.

Zhu, C.; Byrd, R.; Lu, P.; and Nocedal, J. 1997. Algorithm 778: L-BFGS-B: Fortran Subroutines for Large-Scale Bound-Constrained Optimization. *ACM Trans. Math. Softw.*, 23(4): 550–560.

Technical Appendix of paper “Projection-free Graph-based Classifier Learning using Gershgorin Disc Perfect Alignment”

Local Convergence of GDPA Linearization

We discuss convergence to a local minimum via GDPA linearization when solving an optimization $\min_{\mathcal{L} \succeq 0} Q(\mathcal{L})$ where $Q(\mathcal{L})$ is linear. In a topological space [Hausdorff(1957)], a set is a *neighborhood* $V(\mathbf{a})$ of a point \mathbf{a} iff it contains the point \mathbf{a} in its interior—it is an *open set* that contains the point. Given a PSD graph Laplacian $\mathcal{L} \succeq 0$ to a *balanced* signed graph \mathcal{G} , we first define a neighborhood $V_r(\mathcal{L})$ around \mathcal{L} as an *open ball* of radius r centered at \mathcal{L} , i.e., $V_r(\mathcal{L}) \triangleq \{\mathbf{L} \in \mathcal{S}^+ \mid \|\mathcal{L} - \mathbf{L}\|_F^2 < r\}$, where \mathcal{S}^+ is the set of PSD graph Laplacian matrices to balanced graphs of the same edge signs. One can show that \mathcal{S}^+ is a convex cone, and thus given objective $Q(\mathcal{L})$ is also convex, iteratively computing an optimal solution \mathcal{L}^{t+1} in local neighborhood $V_r(\mathcal{L}^t)$ at iteration t would converge to a globally optimal solution as $t \rightarrow \infty$. Since the original feasible space is simply PSD cone $\{\mathbf{L} \mid \mathbf{L} \succeq 0\}$ which contains \mathcal{S}^+ , convergence within \mathcal{S}^+ is a local convergence.

To ensure GDPA linearization computes an optimal solution \mathcal{L}^{t+1} in a well-defined neighborhood $U_\rho(\mathcal{L}^t)$ that approximates $V_r(\mathcal{L}^t)$, we can perform the following procedure¹. First, define $U_\rho(\mathcal{L}^t)$ as the set of matrices satisfying slightly relaxed constraints:

$$\mathcal{L}_{i,i} - \sum_{j \neq i} |s_i \mathcal{L}_{i,j} / s_j| \geq -\rho, \quad \forall i \quad (1)$$

where $\rho > 0$ is a small parameter. Scalars $\{s_i\}$ in (1) are computed from the first eigenvector \mathbf{v} of \mathcal{L}^t as $s_i = v_i^{-1}, \forall i$. For small enough r , matrices $\mathbf{L} \in V_r(\mathcal{L})$ have similar first eigenvectors as \mathbf{v} , and thus constraints (1) would be satisfied. Thus, computing an LP with the relaxed constraints (1) would approximate an optimal solution in $V_r(\mathcal{L}^t)$. There are three possibilities for the obtained solution \mathcal{L}^{t+1} :

1. If $\lambda_{\min}(\mathcal{L}^{t+1}) \geq 0$ and $\mathcal{L}^{t+1} \neq \mathcal{L}^t$, then one can compute new scalars $\{s_i\}$ using the first eigenvector \mathbf{v} of new solution \mathcal{L}^{t+1} , and the algorithm proceeds to the next iteration $t + 1$.
2. If the obtained solution $\lambda_{\min}(\mathcal{L}^{t+1}) \geq 0$ and $\mathcal{L}^{t+1} = \mathcal{L}^t$, then we increase ρ , and the iteration t is repeated.

¹The procedure is applied after the iterations of GDPA linearization return no new solutions \mathcal{L}^{t+1} when setting $\rho = 0$.

3. If $\lambda_{\min}(\mathcal{L}^{t+1}) < 0$, then \mathcal{L}^{t+1} is not a feasible solution, and we decrease ρ , and the iteration t is repeated.

Possibility 1 means that $U_\rho(\mathcal{L}^t)$ is a properly defined neighborhood, since \mathcal{L}^t is not at the set boundary and a new solution $\mathcal{L}^{t+1} \neq \mathcal{L}^t$ is found. Possibility 2 means that $U_\rho(\mathcal{L}^t)$ is not a properly defined neighborhood, since \mathcal{L}^t is at the set boundary. We thus increase ρ to define a larger set $U_\rho(\mathcal{L}^t)$. Possibility 3 means that set $U_\rho(\mathcal{L}^t)$ is too large and includes indefinite matrix \mathcal{L}^{t+1} , and thus ρ is decreased. Note that for possibility 3, $\lambda_{\min}(\mathcal{L}^{t+1}) > -\rho$, since \mathcal{L}^{t+1} is a Laplacian to a balanced graph satisfying (1) using scalars $\{s_i\}$ computed using first eigenvector \mathbf{v} of $\mathcal{L}^t \neq \mathcal{L}^{t+1}$, and thus when its disc left-ends are perfectly aligned, the aligned location must be $> -\rho$.

Note that t is incremented iff $U_\rho(\mathcal{L}^t)$ is a well-defined neighborhood. This means that the only way the algorithm terminates is if after multiple possibility 1, the algorithm repeats possibility 2 and 3 alternately. As the sequence of adjusted ρ becomes increasingly indistinguishable, this would imply we have converged to a local minimum.

Proof of Lemma 2

Proof. Denote by $\mathbf{v} \in \mathbb{R}^N$ the first eigenvector of $\tilde{\mathbf{H}}$. We write

$$\begin{aligned} \mathbf{v}^\top \mathbf{H} \mathbf{v} &= \sum_{(i,j) \in \mathcal{E} \mid 1 \leq i, j \leq N} w_{i,j} (v_i - v_j)^2 + \sum_{i=1}^{N+1} u_i v_i^2 \\ &\quad - \sum_{i=1}^M z_i (v_{N+1} - v_i)^2 \\ \mathbf{v}^\top \tilde{\mathbf{H}} \mathbf{v} &= \sum_{(i,j) \in \mathcal{E} \mid 1 \leq i, j \leq N} w_{i,j} (v_i - v_j)^2 + \sum_{i=1}^{N+1} u_i v_i^2 \\ &\quad + \sum_{i=1}^M (\phi - z_i) (v_{N+1} - v_i)^2 \end{aligned}$$

Given $\phi - z_i > -z_i, \forall i$, $\mathbf{v}^\top \tilde{\mathbf{H}} \mathbf{v} \geq \mathbf{v}^\top \mathbf{H} \mathbf{v}$. Since \mathbf{v} minimizes the Rayleigh quotient of $\tilde{\mathbf{H}}$,

$$\lambda_{\min}(\tilde{\mathbf{H}}) = \frac{\mathbf{v}^\top \tilde{\mathbf{H}} \mathbf{v}}{\mathbf{v}^\top \mathbf{v}} \geq \frac{\mathbf{v}^\top \mathbf{H} \mathbf{v}}{\mathbf{v}^\top \mathbf{v}} \stackrel{(a)}{\geq} \lambda_{\min}(\mathbf{H}). \quad (2)$$

(a) holds since $\lambda_{\min}(\mathbf{H}) = \min_{\mathbf{x}} \frac{\mathbf{x}^\top \mathbf{H} \mathbf{x}}{\mathbf{x}^\top \mathbf{x}}$. \square

Experimental Details for Result Reproduction

We set the convergence threshold of the first eigenvector solver LOBPCG to 10^{-4} as consistent in the LOBPCG literature [Duersch et al.(2018)Duersch, Shao, Yang, and Gu], with maximum number of iterations 200. We set the convergence threshold of our LP solver to be 10^{-4} also, with maximum number of iterations 100, since first-order methods, *i.e.*, CDCS and SD-Cut, aim at computing a solution of moderate accuracy [Zheng, Fantuzzi, and Papachristodoulou(2019)]. Accordingly, we set the convergence threshold of SeDuMi and MOSEK to be ‘low’, which is approximately equal to 10^{-4} and the lowest precision setting in CVX. We set the convergence thresholds of CDCS and SDCut to be 10^{-3} , the maximum number of ADMM iterations in CDCS to be 1000, the maximum number of iterations for L-BFGS-B in SDCut and the main loop in BCR to be 100, and the Frobenius norm weight in SDCut to be 100. We chose these settings since smaller convergence thresholds and larger number of iterations would cause CDCS, SDCut and BCR to be significantly slower to converge. We used default settings for all remaining solvers. All computations were carried out on a Windows 10 64bit PC with AMD Ryzen Threadripper 3960X 24-core processor 3.80 GHz and 128GB of RAM.

We adopted 17 binary datasets that are freely available in UCI [UCI(2021)] and LibSVM [LibSVM(2021)]. For experimental efficiency, we first performed a K -fold ($K \leq 5$) split for each dataset with random seed 0, and then created 10 instances of 50% training-50% test split for each fold, with random seeds 1-10 [Russell and Norvig(2009)]. The above setup resulted in problem sizes from 29 to 400. We applied the following two data normalization schemes for the training/test data: i) a *standardization* scheme in [Dong et al.(2020)Dong, Wang, Yang, and Xue] that first subtracts the mean and divides by the feature-wise standard deviation, and then normalizes to unit length sample-wise, and ii) a *min-max* scheme [Russell and Norvig(2009)] that rescales each feature to within 0 and 1. We added 10^{-12} noise to the dataset to avoid NaN’s due to data normalization on small samples.

Further Experimental Results

We show in Table 1 that SPEC has by far the worst performance in binary signal restoration compared to SDR-based schemes and SNS, demonstrating the limitations of spectral methods in general. Specifically, following an example in [Lam and Liew(2020)], we first corrupted a length- N 1-D signal $[1_{N/2}^\top, -1_{N/2}^\top]$ with iid noise, then solved the optimization $\max_{x_i \in \{-1, 1\}} \mathbf{x}^\top \mathbf{P} \mathbf{x}$, where $\mathbf{P} = [1 \ \mathbf{c}^\top; \mathbf{c} \ \mathbf{W}]$. Here, \mathbf{c} denotes the noisy 1-D signal, and \mathbf{W} denotes the adjacency matrix corresponding to an unweighted line graph. We optimized the above objective using SPEC, SDR primal formulation like (8), SDR dual formulation like (12), modified SDR dual formulation like (20), our proposed GDPA, and SNS. Results were averaged over 100 runs. Table 1 shows that the spectral method SPEC performed by far the worst at all problem sizes ($N = 50, 100, 150$ and 200), types of line graphs (1-hop neighbor and 2-hop neighbor) and noise levels, as observed in previous literature [Guattery and Miller(1998)]. On the other hand, our proposed GDPA performed similarly to the SDR schemes via (8), (12) and (20) and SNS.

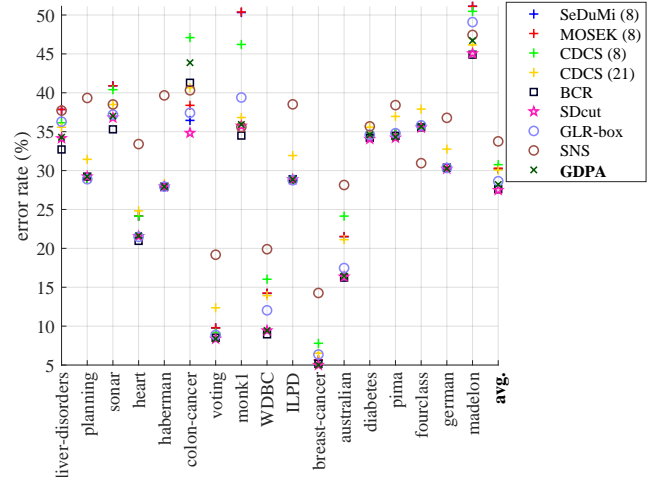


Figure 1: Classification error rates with min-max data re-scaling and problem sizes from 29 to 400.

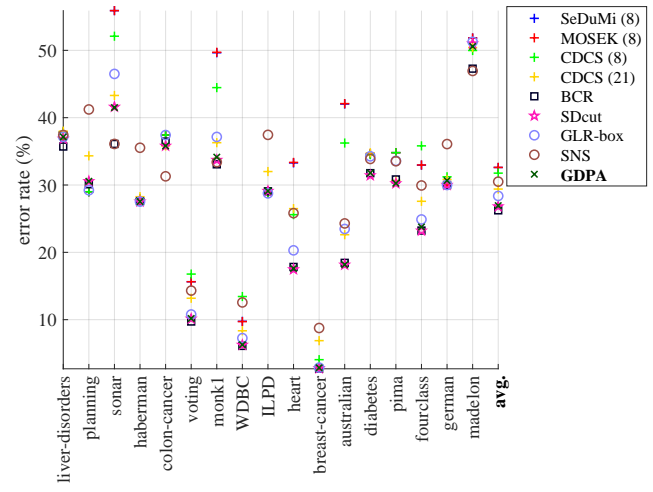


Figure 2: Classification error rates with standardization data re-scaling and problem sizes from 29 to 400.

Fig. 1 and Fig. 2 show the classification error rate with min-max and standardization data re-scaling, respectively. Again, our proposed GDPA linearization (24) closely approximated the modified SDR dual (20) in performance. By factorizing a PSD matrix $\mathbf{M} = \mathbf{X} \mathbf{X}^\top$, BCR avoided tuning of any forward progress step size after a PSD cone projection, which may explain its slightly better performance here. However, BCR solved a non-convex optimization problem converging to a local minimum, and thus occasionally the performance was relatively poor (*e.g.*, see `colon-cancer` in the error rate plots in Fig. 2). Overall, all solvers performed similarly given constructed similarity graphs in the two cases.

Fig. 3 and Fig. 4 show the difference between $\lambda_{\min}(\mathbf{H})$ and $\lambda_{\min}(\tilde{\mathbf{H}})$ described in Lemma 1. On average, the difference between $\lambda_{\min}(\mathbf{H})$ and $\lambda_{\min}(\tilde{\mathbf{H}})$ in Lemma 1 is 1.1608×10^{-7} , which is very small. This demonstrates the tightness of bound $\lambda_{\min}(\tilde{\mathbf{H}}) \leq \lambda_{\min}(\mathbf{H})$ in practice, and thus the effectiveness of Lemma 1.

Table 1: Binary signal restoration error (%). Original signal $[\mathbf{1}_{N/2}^\top, -\mathbf{1}_{N/2}^\top]$ is firstly corrupted using white noise with std σ and then restored using spectral method SPEC, SDP solver SeDuMi on SDR primal in (8), SDR dual in (12), modified SDR dual in (21), proposed GDPA and non-SDR method SNS. Results are averaged over 100 runs.

| N | graph | 1-hop neighbor | | | 2-hop neighbor | | |
|-----|------------------------|----------------|-------|-------|----------------|-------|-------|
| | | σ | 1 | 1.5 | 2 | 1 | 1.5 |
| 50 | SPEC | 11.98 | 23.02 | 29.74 | 8.42 | 19.88 | 27.56 |
| | SDR primal (8) | 3.36 | 12.44 | 22.14 | 2.08 | 7.58 | 15.68 |
| | SDR dual (12) | 3.36 | 12.7 | 22.18 | 1.88 | 6.46 | 14.3 |
| | modified SDR dual (21) | 3.26 | 11.76 | 20.78 | 1.58 | 5.14 | 11.06 |
| | GDPA | 3.56 | 12.16 | 21.44 | 1.92 | 6.34 | 12.72 |
| | SNS | 2.9 | 11.94 | 20.96 | 1.56 | 4.96 | 10.46 |
| 100 | SPEC | 13.04 | 23.24 | 29.59 | 10.02 | 20.94 | 28.06 |
| | SDR primal (8) | 2.45 | 11.96 | 20.82 | 0.90 | 4.82 | 12.92 |
| | SDR dual (12) | 2.28 | 13.68 | 24.28 | 0.77 | 4.44 | 17.80 |
| | modified SDR dual (21) | 2.75 | 10.90 | 19.28 | 0.80 | 3.31 | 8.85 |
| | GDPA | 2.78 | 11.01 | 19.57 | 0.86 | 3.57 | 9.13 |
| | SNS | 1.97 | 11.01 | 19.88 | 0.63 | 2.50 | 8.32 |
| 150 | SPEC | 13.32 | 23.62 | 29.71 | 10.60 | 23.38 | 28.32 |
| | SDR primal (8) | 1.85 | 10.76 | 20.23 | 0.43 | 10.78 | 11.55 |
| | SDR dual (12) | 2.52 | 11.51 | 20.22 | 0.56 | 13.67 | 11.74 |
| | modified SDR dual (21) | 2.43 | 10.60 | 18.85 | 0.50 | 10.68 | 8.33 |
| | GDPA | 2.45 | 10.83 | 19.11 | 0.51 | 10.81 | 8.11 |
| | SNS | 1.73 | 10.89 | 19.76 | 0.31 | 10.92 | 7.19 |
| 200 | SPEC | 13.54 | 23.38 | 29.36 | 11.19 | 21.69 | 28.20 |
| | SDR primal (8) | 1.76 | 10.78 | 19.16 | 0.28 | 3.01 | 10.87 |
| | SDR dual (12) | 2.56 | 13.67 | 24.05 | 0.36 | 3.79 | 14.78 |
| | modified SDR dual (21) | 2.48 | 10.68 | 18.61 | 0.36 | 2.80 | 8.34 |
| | GDPA | 2.46 | 10.81 | 18.67 | 0.39 | 2.83 | 8.52 |
| | SNS | 1.72 | 10.92 | 19.09 | 0.20 | 1.48 | 7.36 |

References

[Dong et al.(2020)] Dong, Wang, Yang, and Xue] Dong, M.; Wang, Y.; Yang, X.; and Xue, J. 2020. Learning Local Metrics and Influential Regions for Classification. *IEEE TPAMI*, 42(6): 1522–1529.

[Duersch et al.(2018)] Duersch, Shao, Yang, and Gu] Duersch, J. A.; Shao, M.; Yang, C.; and Gu, M. 2018. A Robust and Efficient Implementation of LOBPCG. *SIAM Journal on Scientific Computing*, 40(5): C655–C676.

[Guattery and Miller(1998)] Guattery, S.; and Miller, G. L. 1998. On the Quality of Spectral Separators. *SIAM Journal on Matrix Analysis and Applications*, 19(3): 701–719.

[Hausdorff(1957)] Hausdorff, F. 1957. *Set Theory*. Chelsea Publishing Company.

[Lam and Liew(2020)] Lam, B. S.; and Liew, A. W. C. 2020. A Fast Binary Quadratic Programming Solver based on Stochastic Neighborhood Search. *IEEE Transactions on Pattern Analysis and Machine Intelligence*, 1–1.

[LibSVM(2021)] LibSVM. 2021. LibSVM Data: Classification (Binary Class). <https://www.csie.ntu.edu.tw/~cjlin/libsvmtools/datasets/binary.html>. Accessed: 2022-8-15.

[Russell and Norvig(2009)] Russell, S.; and Norvig, P. 2009. *Artificial Intelligence: A Modern Approach*. USA: Prentice Hall Press, 3rd edition. ISBN 0136042597.

[UCI(2021)] UCI. 2021. UCI machine learning repository. <https://archive.ics.uci.edu/ml/datasets.php>. Accessed: 2022-8-15.

[Zheng, Fantuzzi, and Papachristodoulou(2019)] Zheng, Y.; Fantuzzi, G.; and Papachristodoulou, A. 2019. Fast ADMM for Sum-of-Squares Programs Using Partial Orthogonality. *IEEE Transactions on Automatic Control*, 64(9): 3869–3876.

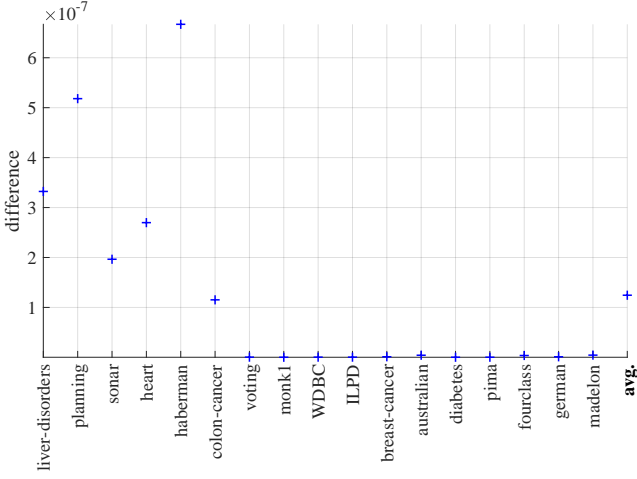


Figure 3: Difference between $\lambda_{\min}(\mathbf{H})$ and $\lambda_{\min}(\bar{\mathbf{H}})$ using GDPA with min-max data re-scaling.

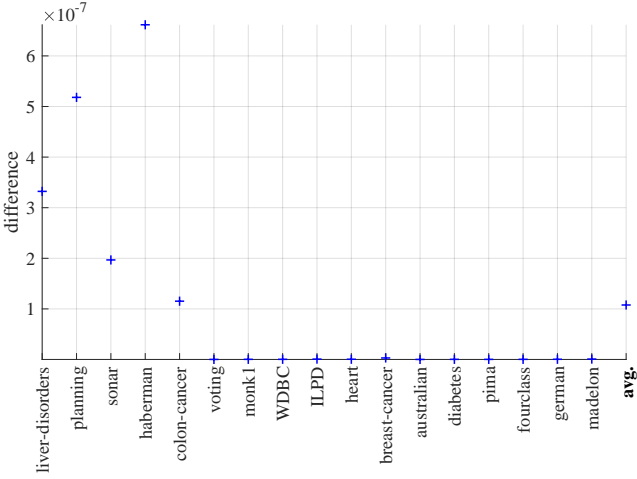


Figure 4: Difference between $\lambda_{\min}(\mathbf{H})$ and $\lambda_{\min}(\bar{\mathbf{H}})$ using GDPA with standardization data re-scaling.